Pasteurella multocidia toxin aggravates ligatured-induced periodontal bone loss and inflammation via NOD-like receptor protein 3 inflammasome

Yineng Han
Peking University School and Hospital of Stomatology
Pengfei Gao
Peking-Tsinghua Center for Life Sciences
Qiaolin Yang
Peking University School and Hospital of Stomatology
Yiping Huang
Peking University School and Hospital of Stomatology
Lingfei Jia
Peking University School and Hospital of Stomatology
Yunfei Zheng
National Center of Stomatology, National Clinical Research Center for Oral Diseases, National Engineering Laboratory for Digital and Material Technology of Stomatology
Weiran Li (weiranli@bjmu.edu.cn)
National Center of Stomatology, National Clinical Research Center for Oral Diseases, National Engineering Laboratory for Digital and Material Technology of Stomatology

Research Article

Keywords: inflammation, periodontitis, inflammasome, Pasteurella multocida toxin, MCC950, NF-κB

Posted Date: March 21st, 2022

DOI: https://doi.org/10.21203/rs.3.rs-1461888/v1

Abstract

NOD-like receptor family pyrin domain containing 3 (NLRP3) inflammasome is reportedly involved in periodontal pathogenesis. *Pasteurella multocida* toxin (PMT) is the major virulence factor of *Pasteurella multocida* strains, which belongs to the GNFR. The existence of GNFR and their toxin may aggravate periodontitis. Therefore, it's important to unclose the regulatory mechanisms of PMT in periodontitis. However, the involvement of NLRP3 inflammasome and PMT in periodontitis remain unclear. The results showed that NLRP3 expression was increased in human and mice gingivae from periodontitis patients and periodontitis mice by immunohistochemical staining and quantitative reverse transcription polymerase chain reaction (qRT-PCR). *Nlrp3*$^{-/-}$ mice showed less periodontal bone loss and lower abundances of *Pasteurella multocida* by 16S rRNA sequencing. PMT promoted NLRP3 expressions by activating nuclear factor kappa light chain enhancer of B cells (NF-κB) pathway and activated NLRP3 inflammasome. This effect was reversed by NLRP3 inhibitor MCC950. Furthermore, PMT aggravated periodontal bone loss and inflammation in WT mice while MCC950 attenuated periodontal bone loss and inflammation. The *Nlrp3*$^{-/-}$ periodontitis models with PMT local injection showed less bone loss and inflammation compared with WT periodontitis mice after PMT treatment. Taken together, our results showed that PMT aggravates periodontal response to the ligature by promoting NLRP3 expression and activating NLRP3 inflammasome, suggesting that NLRP3 may be an effective target for the treatment of periodontitis caused by GNFR and MCC950 may be a potential drug against this disease.

Introduction

Periodontitis is a bacterial-induced chronic inflammatory disease resulting from an imbalance between bacterial antigens and host immune reactions [1, 2]. It affects about 50% of the global population, becoming the sixth most prevalent disease worldwide [3]. The severity of this global oral disease is underscored by the fact that this disease can lead to gingival recession, periodontal tissue destruction, and eventual tooth loss [4]. Periodontitis is mainly caused by gram-negative bacteria. Previous studies have reported NOD-like receptor family pyrin domain-containing 3 (NLRP3) inflammasome plays an important role in the development of periodontitis, and interleukin (IL)-1β expression is higher in the gingival crevicular fluid (GCF), saliva, and gingival tissue of patients with periodontitis than in healthy controls [5-7], indicating that NLRP3 inflammasome is involved in the progression of periodontitis.

NLRP3 inflammasome, a major innate immune sensor, is composed of NLRP3, apoptosis-associated speck-like protein containing a caspase recruitment domain (ASC), and pro-caspase-1. Two signals activate the NLRP3 inflammasome: an initial priming signal 1 and an activation signal 2. Priming signal 1 is initiated by toll-like receptor (TLR) activation, which subsequently activates the nuclear factor kappa light chain enhancer of B cells (NF-κB) pathway, thus inducing the expression of pro-IL-1β, pro-IL-18, and pro-caspase-1. Through activation signal 2, the NLRP3 protein clustering the ASC protein triggers oligomerization of pro-caspase-1, inducing cleavage to form the mature caspase-1 [8]. Active caspase-1 cleaves pro-IL-1β, pro-IL-18, inducing their activation and secretion and recruiting more effector cells to the infection site [9]. Therefore, activated IL-1β is one of important indicators of NLRP3 inflammasome

activation. Recently, a study found that NLRP3 inflammasome mediated elder mice alveolar bone loss and that targeting NLRP3 inflammasome may be a novel option to control periodontal degeneration with age [10].

To date, there are conflicting reports on whether bacteria can activate NLRP3 inflammasome. Some studies found *Porphyromonas gingivalis* (*P.g.*) activates NLRP3 inflammasome in human monocytic-leukemia cells through the TLR2 and TLR4 pathways. [11, 12]. *P.g.* induced the gene expression of IL-1β and intracellular accumulation of IL-1β protein, but it didn't induce the secretion of IL-1β unless subsequent LPS or ATP stimulation. [13]. By contrast, other studies have suggested that *P.g.* inhibits the activation of NLRP3 inflammasomes and plays a counter-regulatory role [14]. Therefore, the role and underlying mechanisms of the NLRP3 inflammasome in periodontitis need further exploration. In present study, *in vivo* experiments revealed lower abundances of *Pasteurella multocida,* which belongs to the non-oral gram-negative facultative rods (GNFR), in *Nlrp3*$^{-/-}$ mice than in WT mice. *In vitro* experiments revealed *Pasteurella multocida* toxin (PMT) significantly promoted NLRP3 expression and activated NLRP3 inflammasome. Moreover, local injection of PMT aggravated ligatured-induced periodontal bone loss and inflammation via NLRP3 inflammasome, while local injection of MCC950 attenuated these effects *in vivo*. These results suggest NLRP3 may be an effective target for the treatment of periodontitis caused by GNFR and that MCC950 may be a potential drug against this disease.

Materials And Methods

Animals

Male, 8-week-old, *Nlrp3*$^{-/-}$ mice and wild-type (WT) C57BL/6 mice were used. *Nlrp3*$^{-/-}$ mice were provided by School of Life Sciences, Peking University (China). WT mice were purchased from WeiTong LiHua Co. (China). Animals were housed at the same time under the same specific-pathogen-free conditions.

Experimental periodontitis and treatment

To build ligature-induced periodontitis model, sterile silk (5-0) was ligatured around the cervical areas of the upper right second molars of mice for one week. Interventions included local injection of the NLRP3 inhibitor MCC950 (MedChemExpress, USA), 10 mg (5ul) twice a day or of PMT (Proteintech Group, USA) 10 nM (5ul) twice a day around the periodontal area. The control group was injected the same volume of normal saline (NS). The injections began on the day that the silks were ligatured (Supplementary Figure 1). All animal experiments protocol was approved by the Experimental Animal Welfare Ethics Branch of Peking University Biomedical Ethics Committee (Protocol LA2020329).

Microbial sample collection and 16S ribosomal RNA (rRNA) sequencing and analysis

After ligature-induced periodontitis for seven days, the silk was removed and transferred into sterile Eppendorf tubes. Then, 200 μL of phosphate-buffered saline (PBS) was added to each tube and shaken for 1 h. The samples were centrifuged at 4 °C for 16S rRNA sequencing.

E.Z.N.A. DNA Kit (Omega Bio-tek, USA) was used to extract microbial genomic DNA according to the manufacturer's instructions. The V3–V4 hypervariable regions of the 16S rRNA gene were subjected to high-throughput sequencing by Beijing Allwegene Tech, Ltd. (China) using the Illumina Miseq PE300 sequencing platform (Illumina, Inc., USA). Quantitative Insights into Microbial Ecology package (v1.2.1) was used for high-quality sequence extraction. UCLUST was used to classify a unique sequence set into an operational taxonomy unit under a 97% identity threshold. Student's t-test was used to calculate alpha- and beta-diversity. The Kruskal-Wallis test was used to determine the significance of categorical variables.

Cell preparation and stimulation

Human monocytes THP-1 were purchased from ScienCell (California, United States) and were cultured in RPMI 1640 supplemented with 10% fetal bovine serum (FBS, Gibco, USA), 100 U/mL penicillin, and 100 μg/mL streptomycin at 37 °C with 5% CO_2. THP-1 cells were differentiated into macrophage-like cells with 50 ng/ml of phorbol 12-mystristate 13-acetate (PMA). The PMA-differentiated THP-1-derived macrophages were stimulated with different concentrations of PMT (0.1, 1, 10 nM) for 6, 12, 24, 36, and 48 h.

GCF collection

GCF collection was performed according to previous study [15]. Briefly, to avoid bleeding, the primary ligature that had been used for periodontitis induction was removed as gently as possible. Then a new, fresh weighed silk thread (about 2 cm in length) was placed around the second molar in each group (Supplementary Figure 2). After 10 min of ligature placement, the silks were removed and weighed using a Mettler Analytical Balance to a sensitivity of 0.05 μg (Mettler Instrument Corporation, USA) to calculate the weight of GCF. Then, the silks were transferred to sterile Eppendorf tubes, and 100 μL of PBS was added to each tube and shaken for 1 h at 4 °C for further analysis.

DNA extraction

Genomic DNA were extracted by using the DNA DNeasy PowerSoil Pro Kits (QIAGEN, Germany) according to manufacturer's instruction. Briefly, the silk containing microbiota and Solution CD1 were added into the PowerBead Pro Tubes and horizontally vortex at maximum speed for 10 min. Then the PowerBead Pro Tubes were centrifuged at 15,000 g for 1 min. The supernatants were transfer to a clean 2 ml tube with 200 μl Solution CD2. The mixture was centrifuge at 15,000 g for 1 min and the supernatants were transferred to another clean 2 ml tubes. 600 μl of Solution CD3 was added and the whole lysate were centrifuged through an MB Spin Column at 15,000 g for 1 min. Then 500 μl of Solution EA and 500 μl of Solution C5 were centrifuged through the MB Spin Column in order. Finally, 50ul of Solution C6 was added to the center of the white filter membrane for centrifugation and 16S rRNA genes from the extracted DNA were quantified by quantitative reverse transcription polymerase chain reaction (qRT-PCR). The primers for *Pasteurella multocidia* and the internal control 16S rDNA were listed in Supplementary Table 1.

qRT-PCR

Total RNA was extracted from the cells and periodontal tissues (gingival tissues and alveolar bone). Gingival tissues around the second molars were collected as gingival samples. Alveolar bone was collected after extraction of the second molar. TRIzol reagent (Invitrogen, USA) was added into these periodontal tissues to fully ground them. Then the procedure was as same as the RNA extraction procedure of cells, which was preformed according to previous study (Han et al., 2020). qRT-PCR was conducted using SYBR Green Master Mix (Roche Applied Science, Switzerland) on an ABI Prism 7500 Real-Time PCR System (Applied Biosystems, USA). The mean of housekeeping gene glyceraldehyde-3-phosphate dehydrogenase (GAPDH) was served as an internal reference. Results were calculated using the $2^{-\Delta\Delta Ct}$ relative expression method. The nucleotide sequences of the primers are listed in Supplementary Table 1.

Western blot

Total protein was extracted using radio immunoprecipitation assay lysis buffer supplemented with a protease inhibitor mixture (Roche Applied Science, Switzerland). Protein concentrations were measured using Pierce BCA Protein Assay Kit (Thermo Scientific, USA) and equal amounts of proteins were separated by sodium dodecyl sulfate-polyacrylamide gel electrophoresis and then transferred onto polyvinylidene fluoride membranes (Merck Millipore, Germany). Primary antibodies against NOD-like receptor family pyrin domain containing 3 (NLRP3, 1:1,000, Proteintech Group), phosphorylated-p65 (1:1,000, Cell Signaling Technology, USA), p65 (1:1,000, Proteintech Group), IκBα (1:1000, Proteintech Group), and β-actin (1:2,000, ZSGB-Bio, China) were incubated overnight at 4 °C. The corresponding secondary antibodies (1:10,000, ZSGB-Bio) were incubated the next day for 1 h. An enhanced chemiluminescence kit (Applygen, China) was used to visualize the protein bands, which were quantified using ImageJ software (http://rsb.info.nih.gov/ij/) [16]. The signals of the target bands were normalized to the β-actin band relative to the control groups.

Enzyme-linked immunosorbent assay (ELISA)

A human IL-1β ELISA kit (Proteintech Group) was used to quantify the inflammatory cytokine IL-1β in the culture supernatant of THP-1-derived macrophages, and a mouse IL-1β ELISA kit (Proteintech Group) was used to quantify the inflammatory cytokine IL-1β in the GCF of mice around the upper second molar according to the manufacturer's instructions. Results were normalized to the cell protein concentrations at an absorbance of 405 nm. The concentrations of IL-1β in GCF were normalized based on the volume of GCF based on the readout from the ELISA kits.

Microcomputed tomography (micro-CT)

To analyze periodontal bone loss after ligation, the fixed mice maxillae were scanned using a Skyscan 1174 micro-CT system (Bruker, Belgium) at a resolution of 10.8 μm. NRecon and CTvox software were used for three-dimensional (3D) reconstruction. Bone volume (BV), bone mineral density (BMD), and bone

volume/tissue volume (BV/TV) ratio were calculated using CTAn software (gray value >1000) by extracting all teeth on the CT data of region of interests according to previous study [17]. The distance between the cemento-enamel junction (CEJ) and the alveolar bone crest (ABC) from each side of the upper second molar (mesial, distal, lingual, and buccal sides) was measured on the sagittal and coronal planes using Data Viewer software.

Human gingival biopsy collection

Human gingival tissues were obtained from patients with periodontitis (n = 12; mean age, 32.4 ± 3.2 years) or from healthy controls who received gingivectomy or crown lengthening during orthodontic or prosthodontic treatment (n = 8; mean age, 31.1 ± 2.8 years). All protocols were approved by the Ethics Committee of Peking University School of Stomatology (PKUSSIRB-201950166), and all patients provided written informed consent. The criteria were formulated according to previous studies [18, 19]. Briefly, samples meeting the criteria that the gingival bleeding index (BI) ≤ 1, periodontal probing depth ≤ 3 mm, no attachment loss, ≥ 20 teeth, and no alveolar bone loss in radiographic examination (the distance between CEJ and ABC ≤ 2 mm) were included in the control group. Samples meeting the criteria that BI ≥ 2, periodontal probing depth ≥ 6 mm, clinical attachment loss ≥ 3 mm and obvious bone loss observed in radiographic examination were included in the periodontitis group. All patients conformed to the criteria of (1) no cigarette smoking; (2) no systematic diseases which might influence periodontal conditions; (3) no anti-inflammatory medications intake during the past 3 months; (4) no periodontal treatment during the past 6 months; (5) not pregnant or breast feeding. All the gingival biopsies were collected from the buccal side. After collection, four control and four periodontitis biopsies were fixed in 4% paraformaldehyde for histological analysis. The other biopsies were used for qRT-PCR analysis.

Histological analysis of periodontal tissue

The specimens (5 μm sections) were stained with hematoxylin and eosin (H&E) staining kit (G1120, Solarbio, China). For immunohistochemical staining, the sections were rehydrated in a graded ethanol series and incubated with an antigen retrieval solution (C1034, Solarbio) for 15 min at 95 °C. Then, sections were incubated with 3% hydrogen peroxide for 10 min at room temperature and incubated with primary antibodies against NLRP3 (1:800, Servicebio, China) and IL-1β (1:800, Servicebio) overnight at 4 °C. Secondary antibodies (ZSGB-Bio) were subsequently applied. After the production of a brown precipitate using a DAB detection kit (Sigma, USA), the sections were counterstained with hematoxylin. Average optical density (Integrated optical density (IOD)/area, AOD) were calculated to analyze the optical density of per unit area in the 400× magnification field.

Statistical analyses

SPSS version 19.0 (IBM, Chicago, IL, USA) was used for statistical analyses. All data are expressed as the mean ± SD of at least three independent experiments. A two-tailed unpaired Student's t-test was used for two-group comparisons. One-way analysis of variance (ANOVA) was used for multiple group comparisons. The threshold of statistical significance was set at $p < 0.05$.

Results

NLRP3 expression is upregulated in periodontitis patients and mice

We first examined the expression of NLRP3 in human gingival tissues to confirm whether its expression was affected by inflammatory states. H&E staining showed that gingival tissue affected by periodontitis had more infiltration of inflammatory cells than those from healthy controls (Figure 1A). Immunohistochemical staining results revealed a higher expression of NLRP3 and IL-1β in gingivae from periodontitis patients than in those from healthy controls (Figure 1A). mRNA expression of NLRP3 and IL-1β were also significantly increased in the diseased group compared to those in the healthy controls (Supplementary Figure 3). H&E staining and micro-CT results showed that ligature-induced periodontitis of the right maxillary second molars had been successfully constructed in mice (Figure 1B, E). BV, BV/TV and BMD were lower in the periodontal group than in the control group (Figure 1C). The distances from CEJ to ABC of the mesial side were calculated using micro-CT analyzing software. The results showed that the CEJ-ABC distance was greater in the periodontal group than in the control group (Figure 1D). The mRNA levels of NLRP3, IL-1β and IL-6 from alveolar bone and gingival tissues were significantly higher in the diseased group than in the control group (Figure 1F). Similarly, immunohistochemistry and semiquantitative analysis (Integrated optical density (IOD)/area) results revealed a higher expression of IL-1β and NLRP3 in the gingival tissues of mice with periodontitis than in the healthy gingivae of WT mice (Figure 1G, H).

NLRP3 deficiency attenuates mice ligatured-induced periodontal bone loss and inflammation *in vivo*

WT (n=5) and *Nlrp3*$^{-/-}$ (n=5) mice were used to explore the role of NLRP3 in the development of ligature-induced periodontitis. Alveolar bone loss was detected via micro-CT and further analyzed by analyzing software. *Nlrp3*$^{-/-}$mice showed less bone loss than WT mice (Figure 2A). The distances between the CEJ and ABC from the mesial side were less in *Nlrp3*$^{-/-}$ mice than in WT mice (Figure 2B). Additionally, BMD, BV and BV/TV were higher in *Nlrp3*$^{-/-}$ mice than in WT mice (Figure 2C). Consistently, H&E staining results showed inflammation and bone resorption were significantly attenuated in *Nlrp3*$^{-/-}$ mice (Figure 2D). Moreover, NLRP3 deficiency remarkably decreased the mRNA expression of the inflammatory cytokines IL-1β and IL-6 (Figure 2E). Immunohistochemistry results further confirmed that NLRP3 deficiency significantly reduced IL-1β expression in gingival tissues of *Nlrp3*$^{-/-}$ mice than in those of WT mice (Figure 2F). Average optical density (IOD)/area) analysis results showed that there were less IL-1β expression in *Nlrp3*$^{-/-}$ mice than in those of WT mice (Figure. 2G).

Altered oral microbiota between WT and *Nlrp3*$^{-/-}$ mice

Previous study reported that NLRP3 knockout increase the capability of macrophage phagocytosis [20]. Therefore, we hypothesized that whether NLRP3 inflammasome influence the oral microbiota, which further influence the progression of periodontitis. Oral microbiota from the silk were collected to analyze the differences in oral bacterial communities between WT (n=3) and *Nlrp3*$^{-/-}$ mice (n=3) with ligature-

induced periodontitis. 16S rRNA gene sequencing analysis revealed that despite individual variations in microbiota, a general discrete clustering pattern of bacterial taxa was depicted between WT and *Nlrp3*$^{-/-}$ mice based on a principal component analysis (Figure 3A). The most significant difference in the microbial abundance between WT and *Nlrp3*$^{-/-}$ mice was *Pasteurella* at the genus level, which was rare in *Nlrp3*$^{-/-}$ mice and enriched in WT mice. To further validate the differentially abundant species we identified according to our 16S rRNA-based microbiome analyses in WT and *Nlrp3*$^{-/-}$ periodontitis mice, we used qRT-PCR to quantify the presence of *Pasteurella multocidia*. The results showed that the fold changes of *Pasteurella multocidia* in *Nlrp3*$^{-/-}$ periodontitis mice were significantly less compared with the WT periodontitis mice (Figure 3B). And the relative abundance analysis results were also consist with the 16S rRNA gene sequencing analysis (Figure 3B).

PMT induces transcription and expression of NLRP3 and inflammatory reaction *in vitro*

We then explored the potential influence of PMT on the progression of periodontitis and investigated whether PMT has an impact on periodontitis via the NLRP3 inflammasome. The mRNA expression of IL-1β, IL-6, and NLRP3 were all significantly upregulated after the stimulation of PMT as well as tumor necrosis factor (TNF), which is an NF-κB pathway agonist in a time-and dose-dependent manner [21] (Figure 3C, Supplementary Figure 4A-C). As the mRNA expression of NLRP3 reached the highest peak at 12 h with 10 nM of both PMT and TNF, we chose 12 h as the stimulation time and 10 nM as the dose in further experiments. Consistently, western blot results also confirmed that PMT exposure induced the protein expression of NLRP3. Similarly, the protein expression of NLRP3 reached the highest peak at 12 h (Figure 3D, Supplementary Figure 4D). We further found that PMT activated the NF-κB signaling pathway and the application of NF-κB inhibitor Bay 11-7082 attenuated PMT-induced NF-κB signaling pathway activity (Figure 3E).

PMT activates NLRP3 inflammasome *in vitro*

We next explored whether PMT participated in the NLRP3 inflammasome activation process. Western blot results showed PMT activated NLRP3 inflammasome with the activation of caspase-1 and the release of activated IL-1β (Figure 4A). However, this effect was significantly inhibited using the NLRP3 inhibitor MCC950 in a dose-dependent manner. Pretreatment with 1 μM MCC950 for 1 h had a minimal effect on PMT-induced NLRP3 inflammasome activation, whereas pretreatment with 10 μM MCC950 significantly reduced the release of activated IL-1β in both whole cell lysates and culture supernatants (Figure 4B). Additionally, MCC950 did not affect NLRP3 protein expression but inhibited NLRP3 inflammasome activation. Furthermore, the time of MCC950 effect against PMT via NLRP3 inhibition was limited. Pretreatment with 10 μM MCC950 significantly reduced the release of activated IL-1β in both whole cell lysates and culture supernatants after 12 h of PMT stimulation. However, MCC950 rarely inhibited NLRP3 inflammasome expression after PMT stimulation for 24 h (Figure 4C). Based on the above data, the regulatory mechanism was deduced in Figure 4D.

MCC950 ameliorates mice periodontal response to the ligature while PMT aggravates mice periodontal response to the ligature

Next, we explore the role of MCC950 and PMT on the progression of periodontitis *in vivo*. Micro-CT reconstruction results demonstrated that MCC950 ameliorated ligature-induced periodontitis, as PMT aggravated ligature-induced periodontitis (Figure 5A). MCC950 treatment significantly improved periodontal bone resorption and inflammation. The ligature-induced periodontitis group synchronously treated with PMT showed a more severe bone loss with less BMD, BV/TV and bone volume than the untreated ligature-induced periodontitis group (Figure 5B). ELISA results revealed that local injection of MCC950 significantly decreased IL-1β protein levels, while PMT remarkably increased IL-1β protein levels in the GCF compared with the control group (Figure 5C). Similarly, both H&E staining and software analysis calculating the distances between the CEJ and ABC from the mesial side showed consistent results (Figure 5D). Immunohistochemical staining results showed that IL-1β expression was significantly higher in the PMT treatment group, while was significantly lower in the MCC950 injection group (Figure 5E). Moreover, we detected the relative expression of *Pasteurella multocidia* via qRT-qPCR of 16s DNA analysis. The results showed that the fold changes of *Pasteurella multocidia* in ligature-induced periodontitis mice after MCC950 treatment were less compared with the WT periodontitis mice group (Supplementary Figure 5A). And the abundance of *Pasteurella multocidia* relative to the total bacteria in ligature-induced periodontitis mice after MCC950 treatment were also less compared with the WT periodontitis mice group (Supplementary Figure 5B).

PMT aggravates periodontitis progression via NLRP3 inflammasome

Then WT and *Nlrp3*$^{-/-}$ mice were used to further verify whether PMT aggravates periodontitis progression via NLRP3 inflammasome. With local intraperitoneal injection of PMT, *Nlrp3*$^{-/-}$ mice showed less bone loss compared to the WT periodontitis mice (Supplementary Figure 6A, B). H&E staining results demonstrated that the perpendicular distance from the mesial and distal ABC to the CEJ was less in *Nlrp3*$^{-/-}$ mice than in the WT periodontitis mice (Supplementary Figure 6A, C). These results suggest that PMT aggravates periodontitis progression via NLRP3 inflammasome.

Discussion

Patients with periodontitis showed higher levels of NLRP3 in the GCF, indicating the important role of NLRP3 in periodontitis progression [22]. NLRP3 inflammasome recognizes various stimuli, such as pathogen-associated molecular patterns [23] and endogenous damage-associated molecular patterns [24]. Periodontal pathogens, including *P.g.*, *Aggregatibacter actinomycetemcomitans* (*A.a.*), and *Fusobacterium nucleatum* (*F.n.*), *Prevotella nigrescens* have been reported to activate the NLRP3 inflammasome, inducing IL-1β secretion [25-27]. Yamaguchi et al. found *Nlrp3*$^{-/-}$ mice showed less alveolar bone resorption with oral *P.g.* injection compared with WT mice [28], indicating that NLRP3 inflammasome is involved in bone metabolism and resorption induced by *P.g.* infection. Consistently, in our study, NLRP3 expression was higher in the gingivae of patients with periodontitis and in ligature-

induced periodontitis in mice. Moreover, NLRP3 deficiency decreased ligature-induced periodontal bone tissue loss and inflammation.

In present study, we used 16S rRNA gene sequencing to detect the oral microbiota after ligature-induced periodontitis for seven days according to previous study [29, 30]. The experimental periods various from 5 days to 60 days [29, 31, 32] and in this study, we found significant alveolar bone loss and inflammatory cells infiltration in the ligature-induced periodontitis group for seven days. Therefore, we chose 7 days for oral microbiota detection. The results showed that the most significant difference in the microbial abundance between WT and *Nlrp3*$^{-/-}$ mice was *Pasteurella* at the genus level. *Pasteurella multocida* is one of the most frequently isolated subgingival non-oral GNFR [33]. It is a commensal bacterium in the gingival crevice of BALB/c mice, nonhuman primates, ferret and dog models [34-37]. At present, most periodontal therapies focus on major periodontopathogens such as *P.g.* and *A.a*. Though GNFR are not always inhabiting the human oral cavity, the existence of *GNFR* and their toxin may resist mechanical debridement from periodontal pockets and are insusceptible to most antibiotics frequently applied in periodontal treatment, even aggravate periodontitis. One of GNFR Neisseria has been reported to be a nitrate-reducing bacteria, promoting endothelial dysfunction, and increased cardiovascular risk [38]. However, the effects of GNFR in the progression of periodontitis remain largely unknown. *Pasteurella multocida* is conserved with *A.a.* and *Haemophilus influenzae*, all belonging to the phylogeny of the *Pasteurellaceae* group. PMT, the major virulence factor produced *by Pasteurella multocida* serotype A and D strains [39], can lead to various pathological processes [40, 41]. One study reported that *A.a.*-immunized mice harboring *Pasteurella* in the oral cavity developed severe periodontitis [35]. In present study, we found PMT significantly aggravated ligature-induced periodontitis *in vivo*. In this study, we didn't explore the role of *Pasteurella multocida* in the progression of periodontitis. In future experiments, the function of *Pasteurella multocida* in the progression of periodontitis and the underlying mechanisms, whether *Pasteurella multocida* activates NLRP3 inflammasome like other periodontal pathogens, and through which signal 1 and signal 2, need to be investigated.

In contrast to lipopolysaccharide, PMT is an AB toxin that can activate the heterotrimeric G proteins Gaq, Ga13, and Gai [42] through deamidation of a glutamine residue required for guanosine triphosphate hydrolysis [43]. A previous study showed PMT stimulates IL-β gene transcription by inducing NF-κB activation; PMT induces IL-1β maturation independent of the NLRP3 inflammasome but dependent on Granzyme A in macrophages [44]. Moreover, the study found this Granzyme A-dependent mechanism is specific for mice macrophages, while human macrophages require NLRP3 inflammasome activation. We found PMT promoted IL-1β and NLRP3 gene transcription via NF-κB pathway activation and stimulated IL-1β secretion via NLRP3 inflammasome activation in human macrophages. Additionally, studies have reported PMT participates in bone homeostasis. It can trigger nuclear factor kappa-B ligand (RANKL)-independent osteoclastogenesis and inhibit osteogenesis via G protein signaling activation [45, 46]. NLRP3 inflammasome has been involved in osteoclastogenesis through IL-1β, which promotes RANKL-induced osteoclast differentiation [47, 48]. NLRP3 inflammasome NLRP3 regulates alveolar bone loss in ligature-induced periodontitis by promoting osteoclastic differentiation [49] and targeting it also reduced

age-related alveolar bone loss [10]. However, whether PMT mediates bone resorption via the NLRP3 inflammasome requires further exploration.

NLRP3 inflammasome was regulated by various factors in periodontitis model to provide therapeutic strategies for periodontitis. Bmi-1 was reported to negatively regulate TLR4-specific activation of the NLRP3 pathway in a mouse model of periodontitis [50]. Oral administration of glyburide significantly suppressed the infiltration of inflammatory cells and the number of osteoclasts in the alveolar bone via targeting the NLRP3 pathway in periodontal diseases [26]. Few NLRP3 inflammasome inhibitors or activators have been reported in regulating the pathogenesis of periodontitis. MCC950 was discovered as a selective small molecule inhibitor of NLRP3 inflammasomes and has been experimentally proven to be beneficial in the control of inflammation and metabolic diseases such as schistosomiasis-induced liver fibrosis, diabetes, and Parkinson's disease [51-53]. MCC950 can directly interact with the NLRP3 NACHT domain to prevent the formation and maintenance of the NLRP3 inflammasome complex. [54, 55]. Our experiments demonstrated MCC950 treatment effectively inhibits PMT-induced NLRP3 inflammasome activation and further suppresses IL-1β production in a concentration-dependent manner *in vitro*. However, MCC950 are high cost and short half-life [56] and the development of more potent agents will offer insights into immune-mediated periodontitis strategies in future.

The limitation of this study was that we didn't unclose why there was less *Pasteurella* in *Nlrp3*$^{-/-}$ periodontitis mice. Taxman et al once provided a novel mechanism of pathogen-mediated inflammasome inhibition through the suppression of endocytosis. *P.g.* repressed NLRP3 inflammasome activation through endocytosis [14]. Moreover, Sun et al found that loss of PCSK9 helped maintain a normal symbiotic microbiota and to eliminate pathogen lipid. PCSK9 knockout enhanced the ability of BMMs to phagocytose *P.g*. [57]. We hypothesized that NLRP3 inflammasome may also affect the endocytosis on Pasteurella. However, further experiments were needed to verify this hypothesis.

In conclusion, we confirmed there were lower abundances of *Pasteurella multocida* in *Nlrp3*$^{-/-}$ periodontitis mice than in WT periodontitis mice. PMT not only promoted NLRP3 expressions by activating NF-κB signaling pathway, but also effectively activated NLRP3 inflammasome to further trigger pro-IL-1β cleavage *in vitro.* PMT aggravated ligatured-induced periodontal bone loss and inflammation via NLRP 3 inflammasome and this effect was significantly reversed by NLRP3 inhibitor MCC950 with reduced IL-1β activation. Our findings enriched the understanding of NLRP3 inflammasome in the presence of GNFR during periodontitis progression. Furthermore, our findings provided a possibility that targeting NLRP3 inflammasome can alleviate PMT-induced periodontitis and that MCC950 can be a novel option to control periodontal diseases.

Abbreviations

A.a. = Aggregatibacter actinomycetemcomitans; ABC = alveolar bone crest; ANOVA = analysis of variance; ASC = apoptosis-associated speck-like protein containing a CARD; BI = bleeding index; BMD = bone mineral density; BV = bone volume; BV/TV = bone volume/tissue volume; CEJ = cementum-enamel

junction; EDTA = ethylene diamine tetraacetic acid; ELISA = Enzyme-linked immunosorbent assay; *F.n =Fusobacterium nucleatum*; GAPDH = glyceraldehyde-3-phosphate dehydrogenase; GCF = gingival crevicular fluid; GNFR = non-oral gram-negative facultative rods; H&E = hematoxylin and eosin; IL = interleukin; IOD integrated optical density; LPS = lipopolysaccharide; micro-CT = microcomputed tomography; mRNA = messenger RNA; NLRP3 = NOD-like receptor family pyrin domain containing 3; NF-κB = nuclear factor kappa light chain enhancer of B cells; NS = normal saline; PBS = phosphate-buffered saline; *P.g. = Porphyromonas gingivalis*; PMA = phorbol 12-mystristate 13-acetate; PMT *= Pasteurella multocida* toxin QIIME = quantitative insights into microbial ecology; qRT-PCR = quantitative reverse-transcription polymerase chain reaction; RANKL= nuclear factor kappa-B ligand; Sup = supernatants; TLR = toll-like receptor; TNF = tumor necrosis factor; WCL = whole cell lysates; 3D = three-dimensional.

Declarations

Disclosure of potential conflicts of interests

The authors declare no conflicts of interest.

Data availability statement

The data that support the findings of this study are available on request from the corresponding author.

Funding

This study was financially supported by grants from the National Natural Science Foundation of China (No. 82071119, 82071142).

Ethics approval

All animal experiments protocol was approved by the Experimental Animal Welfare Ethics Branch of Peking University Biomedical Ethics Committee (Protocol LA2020329).

References

1. Petersen PE and Ogawa H (2012) The global burden of periodontal disease: towards integration with chronic disease prevention and control. Periodontol 2000 60:15-39. doi: 10.1111/j.1600-0757.2011.00425.x

2. Kuula H, Salo T, Pirila E, Tuomainen AM, Jauhiainen M, Uitto VJ, Tjaderhane L, Pussinen PJ and Sorsa T (2009) Local and systemic responses in matrix metalloproteinase 8-deficient mice during Porphyromonas gingivalis-induced periodontitis. Infect Immun 77:850-9. doi: 10.1128/IAI.00873-08

3. West NX (2019) Living with periodontitis. Br Dent J 227:537. doi: 10.1038/s41415-019-0838-x

4. Renn TY, Huang YK, Feng SW, Wang HW, Lee WF, Lin CT, Burnouf T, Chen LY, Kao PF and Chang HM (2018) Prophylactic supplement with melatonin successfully suppresses the pathogenesis of periodontitis through normalizing RANKL/OPG ratio and depressing the TLR4/MyD88 signaling pathway. J Pineal Res 64. doi: 10.1111/jpi.12464

5. Garcia-Hernandez AL, Munoz-Saavedra AE, Gonzalez-Alva P, Moreno-Fierros L, Llamosas-Hernandez FE, Cifuentes-Mendiola SE and Rubio-Infante N (2019) Upregulation of proteins of the NLRP3 inflammasome in patients with periodontitis and uncontrolled type 2 diabetes. Oral Dis 25:596-608. doi: 10.1111/odi.13003

6. Huang X, Yang X, Ni J, Xie B, Liu Y, Xuan D and Zhang J (2015) Hyperglucose contributes to periodontitis: involvement of the NLRP3 pathway by engaging the innate immunity of oral gingival epithelium. J Periodontol 86:327-35. doi: 10.1902/jop.2014.140403

7. Tobon-Arroyave SI, Jaramillo-Gonzalez PE and Isaza-Guzman DM (2008) Correlation between salivary IL-1beta levels and periodontal clinical status. Arch Oral Biol 53:346-52. doi: 10.1016/j.archoralbio.2007.11.005

8. Yang X, Chang HY and Baltimore D (1998) Autoproteolytic activation of pro-caspases by oligomerization. Mol Cell 1:319-25. doi: 10.1016/s1097-2765(00)80032-5

9. Martinon F, Burns K and Tschopp J (2002) The inflammasome: a molecular platform triggering activation of inflammatory caspases and processing of proIL-beta. Mol Cell 10:417-26. doi: 10.1016/s1097-2765(02)00599-3

10. Zang Y, Song JH, Oh SH, Kim JW, Lee MN, Piao X, Yang JW, Kim OS, Kim TS, Kim SH and Koh JT (2020) Targeting NLRP3 Inflammasome Reduces Age-Related Experimental Alveolar Bone Loss. J Dent Res 99:1287-1295. doi: 10.1177/0022034520933533

11. Park E, Na HS, Song YR, Shin SY, Kim YM and Chung J (2014) Activation of NLRP3 and AIM2 inflammasomes by Porphyromonas gingivalis infection. Infect Immun 82:112-23. doi: 10.1128/IAI.00862-13

12. Bostanci N, Emingil G, Saygan B, Turkoglu O, Atilla G, Curtis MA and Belibasakis GN (2009) Expression and regulation of the NALP3 inflammasome complex in periodontal diseases. Clin Exp Immunol 157:415-22. doi: 10.1111/j.1365-2249.2009.03972.x

13. Yilmaz O, Sater AA, Yao L, Koutouzis T, Pettengill M and Ojcius DM (2010) ATP-dependent activation of an inflammasome in primary gingival epithelial cells infected by Porphyromonas gingivalis. Cell Microbiol 12:188-98. doi: 10.1111/j.1462-5822.2009.01390.x

14. Taxman DJ, Swanson KV, Broglie PM, Wen H, Holley-Guthrie E, Huang MT, Callaway JB, Eitas TK, Duncan JA and Ting JP (2012) Porphyromonas gingivalis mediates inflammasome repression in

polymicrobial cultures through a novel mechanism involving reduced endocytosis. J Biol Chem 287:32791-9. doi: 10.1074/jbc.M112.401737

15. Matsuda S, Movila A, Suzuki M, Kajiya M, Wisitrasameewong W, Kayal R, Hirshfeld J, Al-Dharrab A, Savitri IJ, Mira A, Kurihara H, Taubman MA and Kawai T (2016) A novel method of sampling gingival crevicular fluid from a mouse model of periodontitis. J Immunol Methods 438:21-25. doi: 10.1016/j.jim.2016.08.008

16. Goto M (2019) [8. Image Processing Using ImageJ]. Nihon Hoshasen Gijutsu Gakkai Zasshi 75:688-692. doi: 10.6009/jjrt.2019_JSRT_75.7.688

17. Kure K, Sato H, Suzuki JI, Itai A, Aoyama N and Izumi Y (2019) A novel IkB kinase inhibitor attenuates ligature-induced periodontal disease in mice. J Periodontal Res 54:164-173. doi: 10.1111/jre.12615

18. Garaicoa-Pazmino C, Fretwurst T, Squarize CH, Berglundh T, Giannobile WV, Larsson L and Castilho RM (2019) Characterization of macrophage polarization in periodontal disease. J Clin Periodontol 46:830-839. doi: 10.1111/jcpe.13156

19. Wu X, Chen H, Wang Y and Gu Y (2020) Akt2 Affects Periodontal Inflammation via Altering the M1/M2 Ratio. J Dent Res 99:577-587. doi: 10.1177/0022034520910127

20. Hu X, Jia X, Xu C, Wei Y, Wang Z, Liu G, You Q, Lu G and Gong W (2021) Downregulation of NK cell activities in Apolipoprotein C-III-induced hyperlipidemia resulting from lipid-induced metabolic reprogramming and crosstalk with lipid-laden dendritic cells. Metabolism 120:154800. doi: 10.1016/j.metabol.2021.154800

21. Vince JE, Pantaki D, Feltham R, Mace PD, Cordier SM, Schmukle AC, Davidson AJ, Callus BA, Wong WW, Gentle IE, Carter H, Lee EF, Walczak H, Day CL, Vaux DL and Silke J (2009) TRAF2 must bind to cellular inhibitors of apoptosis for tumor necrosis factor (tnf) to efficiently activate nf-{kappa}b and to prevent tnf-induced apoptosis. J Biol Chem 284:35906-15. doi: 10.1074/jbc.M109.072256

22. Yu L, Zhou C, Wei Z and Shi Z (2019) Effect of combined periodontal-orthodontic treatment on NOD-like receptor protein 3 and high mobility group box-1 expressions in patients with periodontitis and its clinical significance. Medicine (Baltimore) 98:e17724. doi: 10.1097/MD.0000000000017724

23. Lamkanfi M and Dixit VM (2014) Mechanisms and functions of inflammasomes. Cell 157:1013-22. doi: 10.1016/j.cell.2014.04.007

24. Wen H, Miao EA and Ting JP (2013) Mechanisms of NOD-like receptor-associated inflammasome activation. Immunity 39:432-41. doi: 10.1016/j.immuni.2013.08.037

25. Shibata K (2018) Historical aspects of studies on roles of the inflammasome in the pathogenesis of periodontal diseases. Mol Oral Microbiol 33:203-211. doi: 10.1111/omi.12217

26. Kawahara Y, Kaneko T, Yoshinaga Y, Arita Y, Nakamura K, Koga C, Yoshimura A and Sakagami R (2020) Effects of Sulfonylureas on Periodontopathic Bacteria-Induced Inflammation. J Dent Res 99:830-838. doi: 10.1177/0022034520913250

27. Jang HM, Park JY, Lee YJ, Kang MJ, Jo SG, Jeong YJ, Cho NP, Cho SD, Kim DJ and Park JH (2021) TLR2 and the NLRP3 inflammasome mediate IL-1beta production in Prevotella nigrescens-infected dendritic cells. Int J Med Sci 18:432-440. doi: 10.7150/ijms.47197

28. Yamaguchi Y, Kurita-Ochiai T, Kobayashi R, Suzuki T and Ando T (2017) Regulation of the NLRP3 inflammasome in Porphyromonas gingivalis-accelerated periodontal disease. Inflamm Res 66:59-65. doi: 10.1007/s00011-016-0992-4

29. Johnstone KF, Wei Y, Bittner-Eddy PD, Vreeman GW, Stone IA, Clayton JB, Reilly CS, Walbon TB, Wright EN, Hoops SL, Boyle WS, Costalonga M and Herzberg MC (2021) Calprotectin (S100A8/A9) Is an Innate Immune Effector in Experimental Periodontitis. Infect Immun 89:e0012221. doi: 10.1128/IAI.00122-21

30. Sato K, Yamazaki K, Kato T, Nakanishi Y, Tsuzuno T, Yokoji-Takeuchi M, Yamada-Hara M, Miura N, Okuda S, Ohno H and Yamazaki K (2021) Obesity-Related Gut Microbiota Aggravates Alveolar Bone Destruction in Experimental Periodontitis through Elevation of Uric Acid. mBio 12:e0077121. doi: 10.1128/mBio.00771-21

31. Kim JW, Jung BH, Lee JH, Yoo KY, Lee H, Kang MS and Lee JK (2020) Effect of Weissella cibaria on the reduction of periodontal tissue destruction in mice. J Periodontol 91:1367-1374. doi: 10.1002/JPER.19-0288

32. de Molon RS, Mascarenhas VI, de Avila ED, Finoti LS, Toffoli GB, Spolidorio DM, Scarel-Caminaga RM, Tetradis S and Cirelli JA (2016) Long-term evaluation of oral gavage with periodontopathogens or ligature induction of experimental periodontal disease in mice. Clin Oral Investig 20:1203-16. doi: 10.1007/s00784-015-1607-0

33. van Winkelhoff AJ, Rurenga P, Wekema-Mulder GJ, Singadji ZM and Rams TE (2016) Non-oral gram-negative facultative rods in chronic periodontitis microbiota. Microb Pathog 94:117-22. doi: 10.1016/j.micpath.2016.01.020

34. Fischer RG, Edwardsson S and Klinge B (1994) Oral microflora of the ferret at the gingival sulcus and mucosa membrane in relation to ligature-induced periodontitis. Oral Microbiol Immunol 9:40-9. doi: 10.1111/j.1399-302x.1994.tb00213.x

35. Kawai T, Paster BJ, Komatsuzawa H, Ernst CW, Goncalves RB, Sasaki H, Ouhara K, Stashenko PP, Sugai M and Taubman MA (2007) Cross-reactive adaptive immune response to oral commensal bacteria results in an induction of receptor activator of nuclear factor-kappaB ligand (RANKL)-dependent periodontal bone resorption in a mouse model. Oral Microbiol Immunol 22:208-15. doi: 10.1111/j.1399-302X.2007.00348.x

36. Radice M, Martino PA and Reiter AM (2006) Evaluation of subgingival bacteria in the dog and susceptibility to commonly used antibiotics. J Vet Dent 23:219-24. doi: 10.1177/089875640602300404

37. Ebersole J, Kirakodu S, Chen J, Nagarajan R and Gonzalez OA (2020) Oral Microbiome and Gingival Transcriptome Profiles of Ligature-Induced Periodontitis. J Dent Res 99:746-757. doi: 10.1177/0022034520906138

38. Pignatelli P, Fabietti G, Ricci A, Piattelli A and Curia MC (2020) How Periodontal Disease and Presence of Nitric Oxide Reducing Oral Bacteria Can Affect Blood Pressure. Int J Mol Sci 21. doi: 10.3390/ijms21207538

39. Harper M, Boyce JD and Adler B (2006) Pasteurella multocida pathogenesis: 125 years after Pasteur. FEMS Microbiol Lett 265:1-10. doi: 10.1111/j.1574-6968.2006.00442.x

40. Latz E, Xiao TS and Stutz A (2013) Activation and regulation of the inflammasomes. Nat Rev Immunol 13:397-411. doi: 10.1038/nri3452

41. Kubatzky KF, Kloos B and Hildebrand D (2013) Signaling cascades of Pasteurella multocida toxin in immune evasion. Toxins (Basel) 5:1664-81. doi: 10.3390/toxins5091664

42. Orth JH, Fester I, Siegert P, Weise M, Lanner U, Kamitani S, Tachibana T, Wilson BA, Schlosser A, Horiguchi Y and Aktories K (2013) Substrate specificity of Pasteurella multocida toxin for alpha subunits of heterotrimeric G proteins. FASEB J 27:832-42. doi: 10.1096/fj.12-213900

43. Orth JH, Preuss I, Fester I, Schlosser A, Wilson BA and Aktories K (2009) Pasteurella multocida toxin activation of heterotrimeric G proteins by deamidation. Proc Natl Acad Sci U S A 106:7179-84. doi: 10.1073/pnas.0900160106

44. Hildebrand D, Bode KA, Riess D, Cerny D, Waldhuber A, Rommler F, Strack J, Korten S, Orth JH, Miethke T, Heeg K and Kubatzky KF (2014) Granzyme A produces bioactive IL-1beta through a nonapoptotic inflammasome-independent pathway. Cell Rep 9:910-7. doi: 10.1016/j.celrep.2014.10.003

45. Ebner JK, Konig GM, Kostenis E, Siegert P, Aktories K and Orth JHC (2019) Activation of Gq signaling by Pasteurella multocida toxin inhibits the osteoblastogenic-like actions of Activin A in C2C12 myoblasts, a cell model of fibrodysplasia ossificans progressiva. Bone 127:592-601. doi: 10.1016/j.bone.2019.07.031

46. Chakraborty S, Kloos B, Harre U, Schett G and Kubatzky KF (2017) Pasteurella multocida Toxin Triggers RANKL-Independent Osteoclastogenesis. Front Immunol 8:185. doi: 10.3389/fimmu.2017.00185

47. Kim JH, Jin HM, Kim K, Song I, Youn BU, Matsuo K and Kim N (2009) The mechanism of osteoclast differentiation induced by IL-1. J Immunol 183:1862-70. doi: 10.4049/jimmunol.0803007

48. Khajuria DK, Patil ON, Karasik D and Razdan R (2018) Development and evaluation of novel biodegradable chitosan based metformin intrapocket dental film for the management of periodontitis and alveolar bone loss in a rat model. Arch Oral Biol 85:120-129. doi: 10.1016/j.archoralbio.2017.10.009

49. Chen Y, Yang Q, Lv C, Chen Y, Zhao W, Li W, Chen H, Wang H, Sun W and Yuan H (2021) NLRP3 regulates alveolar bone loss in ligature-induced periodontitis by promoting osteoclastic differentiation. Cell Prolif 54:e12973. doi: 10.1111/cpr.12973

50. Qin ZY, Gu X, Chen YL, Liu JB, Hou CX, Lin SY, Hao NN, Liang Y, Chen W and Meng HY (2021) Tolllike receptor 4 activates the NLRP3 inflammasome pathway and periodontal inflammaging by inhibiting Bmi1 expression. Int J Mol Med 47:137-150. doi: 10.3892/ijmm.2020.4787

51. Gordon R, Albornoz EA, Christie DC, Langley MR, Kumar V, Mantovani S, Robertson AAB, Butler MS, Rowe DB, O'Neill LA, Kanthasamy AG, Schroder K, Cooper MA and Woodruff TM (2018) Inflammasome inhibition prevents alpha-synuclein pathology and dopaminergic neurodegeneration in mice. Sci Transl Med 10. doi: 10.1126/scitranslmed.aah4066

52. Zhang WJ, Fang ZM and Liu WQ (2019) NLRP3 inflammasome activation from Kupffer cells is involved in liver fibrosis of Schistosoma japonicum-infected mice via NF-kappaB. Parasit Vectors 12:29. doi: 10.1186/s13071-018-3223-8

53. Hull C, Dekeryte R, Buchanan H, Kamli-Salino S, Robertson A, Delibegovic M and Platt B (2020) NLRP3 inflammasome inhibition with MCC950 improves insulin sensitivity and inflammation in a mouse model of frontotemporal dementia. Neuropharmacology 180:108305. doi: 10.1016/j.neuropharm.2020.108305

54. Coll RC, Hill JR, Day CJ, Zamoshnikova A, Boucher D, Massey NL, Chitty JL, Fraser JA, Jennings MP, Robertson AAB and Schroder K (2019) MCC950 directly targets the NLRP3 ATP-hydrolysis motif for inflammasome inhibition. Nat Chem Biol 15:556-559. doi: 10.1038/s41589-019-0277-7

55. Tapia-Abellan A, Angosto-Bazarra D, Martinez-Banaclocha H, de Torre-Minguela C, Ceron-Carrasco JP, Perez-Sanchez H, Arostegui JI and Pelegrin P (2019) MCC950 closes the active conformation of NLRP3 to an inactive state. Nat Chem Biol 15:560-564. doi: 10.1038/s41589-019-0278-6

56. Coll RC, Robertson AA, Chae JJ, Higgins SC, Munoz-Planillo R, Inserra MC, Vetter I, Dungan LS, Monks BG, Stutz A, Croker DE, Butler MS, Haneklaus M, Sutton CE, Nunez G, Latz E, Kastner DL, Mills KH, Masters SL, Schroder K, Cooper MA and O'Neill LA (2015) A small-molecule inhibitor of the NLRP3 inflammasome for the treatment of inflammatory diseases. Nat Med 21:248-55. doi: 10.1038/nm.3806

57. Sun HL, Wu YR, Song FF, Gan J, Huang LY, Zhang L and Huang C (2018) Role of PCSK9 in the Development of Mouse Periodontitis Before and After Treatment: A Double-Edged Sword. J Infect Dis 217:667-680. doi: 10.1093/infdis/jix574

Figures

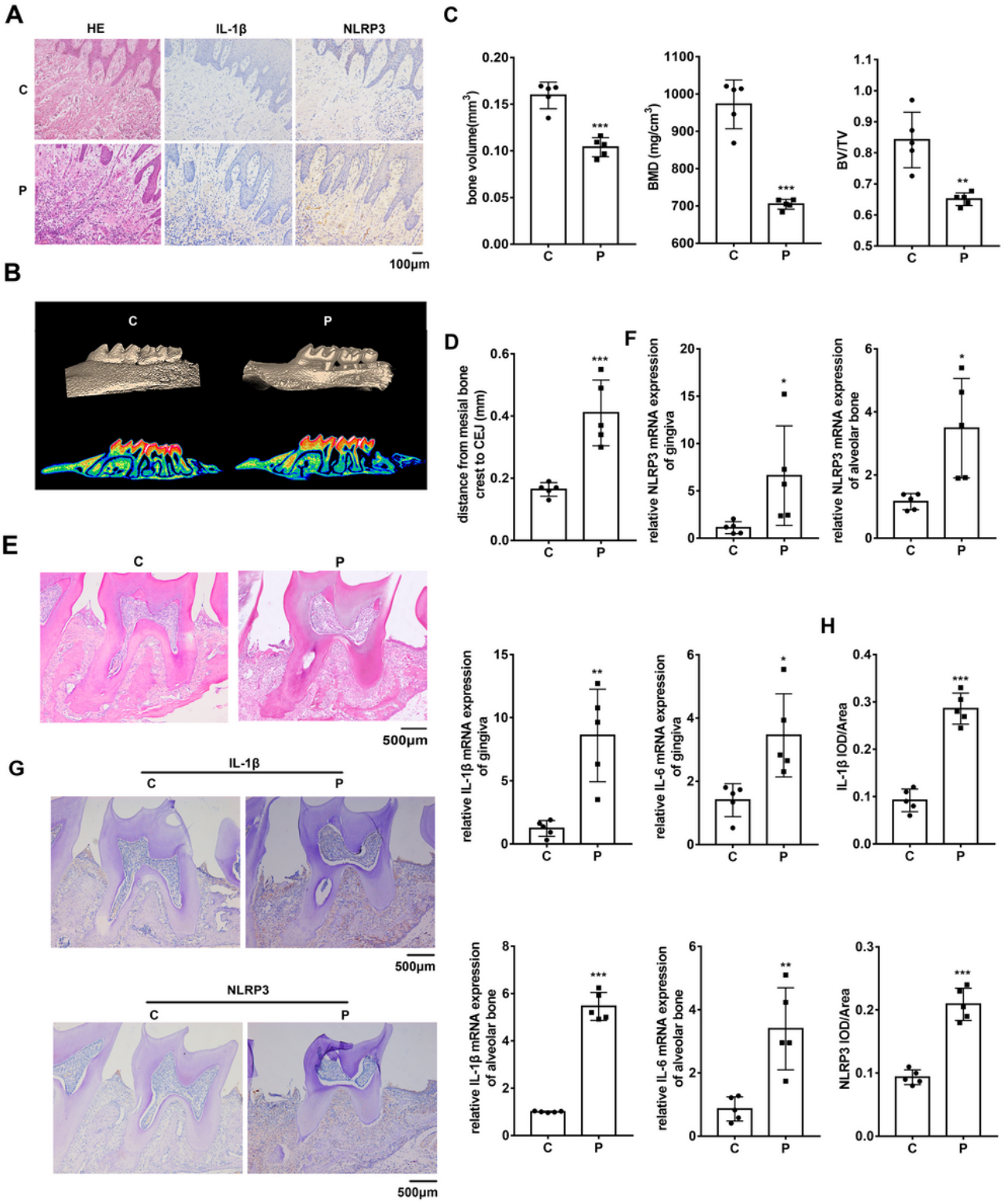

Figure 1

NLRP3 expression is upregulated in periodontitis patients and mice. (A) Immunohistochemistry staining of IL-1β and NLRP3 in gingivae from healthy and periodontitis individuals. (B) Reconstructed 3D micro-CT images of control, and periodontitis groups. (C) BV, BV/TV, and BMD analysis of control, and periodontitis groups (n=5/group). (D) The distances between the CEJ and the ABC from the mesial side of control, and periodontitis groups (n=5/group). (E, G) H&E staining and immunohistochemistry staining

of IL-1β and NLRP3 in the gingivae in control and periodontitis groups. The histogram shows the quantification of positive cells (n=5/group). (F) mRNA expression of IL-1β, IL-6, IL-10 and NLRP3 in control and periodontitis groups by qRT-PCR (n=5/group). GAPDH was used for normalization relative to control groups. (H) Quantitative analysis (Integrated optical density (IOD)/Area) of IL-1β and NLRP3 immunohistochemistry staining of control and periodontitis groups. Values are presented as mean ± SD. (*p<0.05, **p<0.01, *** p<0.001). Abbreviations: ABC = alveolar bone crest; BMD = bone mineral density; BV = bone volume; BV/TV = bone volume/tissue volume ratio; CEJ = cemento-enamel junction; GAPDH = glyceraldehyde-3-phosphate dehydrogenase; H&E = hematoxylin and eosin; IL = interleukin; micro-CT = microcomputed tomography; mRNA = messenger RNA; NLRP3 = NOD-like receptor family pyrin domain containing 3; qRT-PCR = quantitative reverse transcription polymerase chain reaction; 3D = three-dimensional.

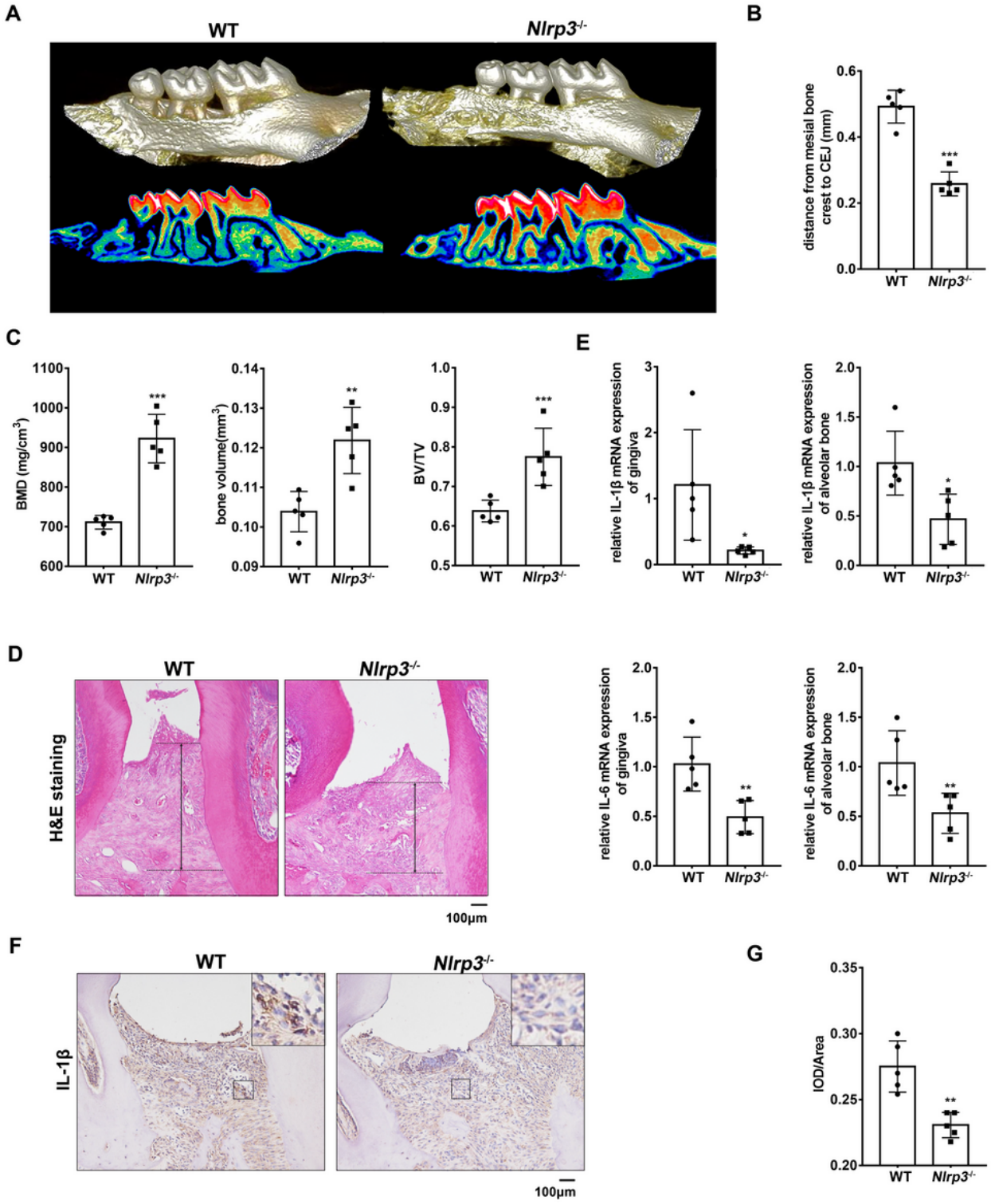

Figure 2

NLRP3 deficiency attenuates mice periodontitis *in vivo*. (A) Reconstructed 3D micro-CT images of periodontitis models of WT and *Nlrp3*$^{-/-}$ mice. (B) The distances between the CEJ and the ABC from the mesial side of upper right second molars of WT and *Nlrp3*$^{-/-}$ mice (n=5/group). (C) BMD, BV, BV/TV and resorbed bone volume analysis of WT and *Nlrp3*$^{-/-}$ mice (n=5/group). (D, F, G) H&E staining and

immunohistochemistry staining of IL-1β of WT and *Nlrp3*$^{-/-}$ mice. The histogram shows the quantification of average optical density (Integrated optical density (IOD)/Area) of IL-1β immunohistochemistry staining of WT and *Nlrp3*$^{-/-}$ mice groups (n=5/group). (E) mRNA expression of IL-1β and IL-6 in the gingiva and alveolar bone of WT and *Nlrp3*$^{-/-}$ mice (n=5/group) by qRT-PCR. GAPDH was used for normalization relative to control groups. Values are presented as mean ± SD. (**p*<0.05, ** *p*<0.01, *** *p*<0.001). Abbreviations: ABC = alveolar bone crest; BMD = bone mineral density; BV = bone volume; BV/TV = bone volume/tissue volume ratio; CEJ = cemento-enamel junction; GAPDH = glyceraldehyde-3-phosphate dehydrogenase; H&E = hematoxylin and eosin; IL = interleukin; micro-CT = microcomputed tomography; mRNA = messenger RNA; NLRP3 = NOD-like receptor family pyrin domain containing 3; qRT-PCR = quantitative reverse transcription polymerase chain reaction; 3D = three-dimensional.

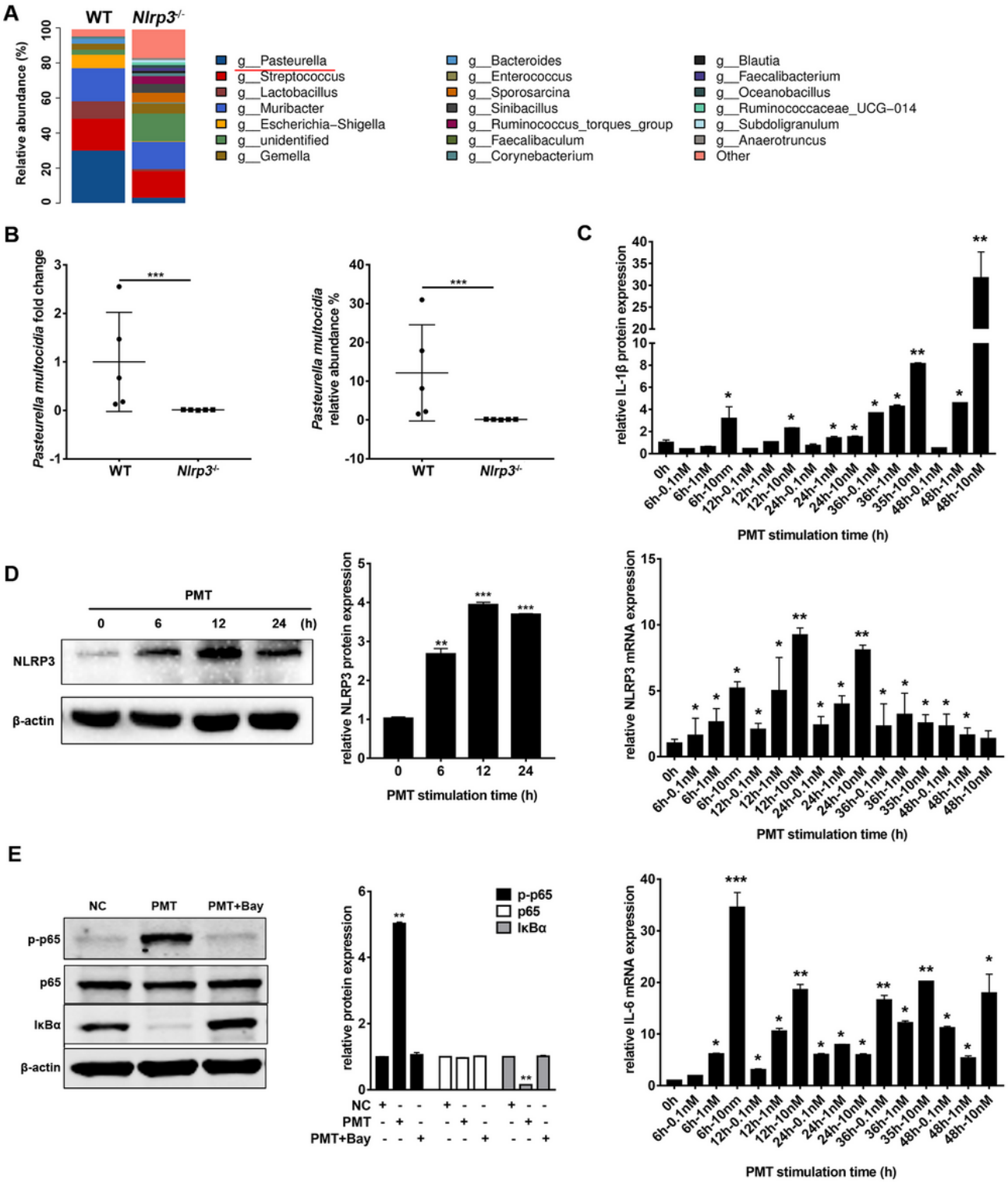

Figure 3

Altered Oral Microbiota between WT and *Nlrp3*$^{-/-}$ mice and PMT induces transcription and expression of NLRP3 and inflammatory reaction *in vitro*. (A)16S rRNA gene sequencing analysis show the general discrete clustering pattern of bacterial taxa between WT and *Nlrp3*$^{-/-}$ mice (n=3/group). (B) qRT-PCR validation of *Pasteurella multocidia* in WT and *Nlrp3*$^{-/-}$ mice (n=5/group). (C) mRNA expression of IL-1β, IL-6 and NLRP3 after the stimulation of PMT at a series of time by qRT-PCR (n=5/group). GAPDH was

used for normalization relative to control groups. (D) Protein expression of NLRP3 and the internal control β-actin after the stimulation of PMT at a series of time by western blot. The histogram shows the quantification of band intensities. β-actin was used for normalization relative to the control groups. (E) Protein expression of pp65, p65, IκBα and the internal control β-actin after stimulation of PMT with or without pre-treatment of NF-κB inhibitor Bay 11-7082 by western blot. The histogram shows the quantification of band intensities. β-actin was used for normalization relative to the control groups. Values are presented as mean ± SD. (*p<0.05, **p<0.01, ***p<0.001). Abbreviations: GAPDH = glyceraldehyde-3-phosphate dehydrogenase; IL = interleukin; mRNA = messenger RNA; NLRP3 = NOD-like receptor family pyrin domain containing 3; NF-κB = nuclear factor kappa light chain enhancer of B cells; PMT = *Pasteurella multocida* toxin; qRT-PCR = quantitative reverse-transcription polymerase chain reaction.

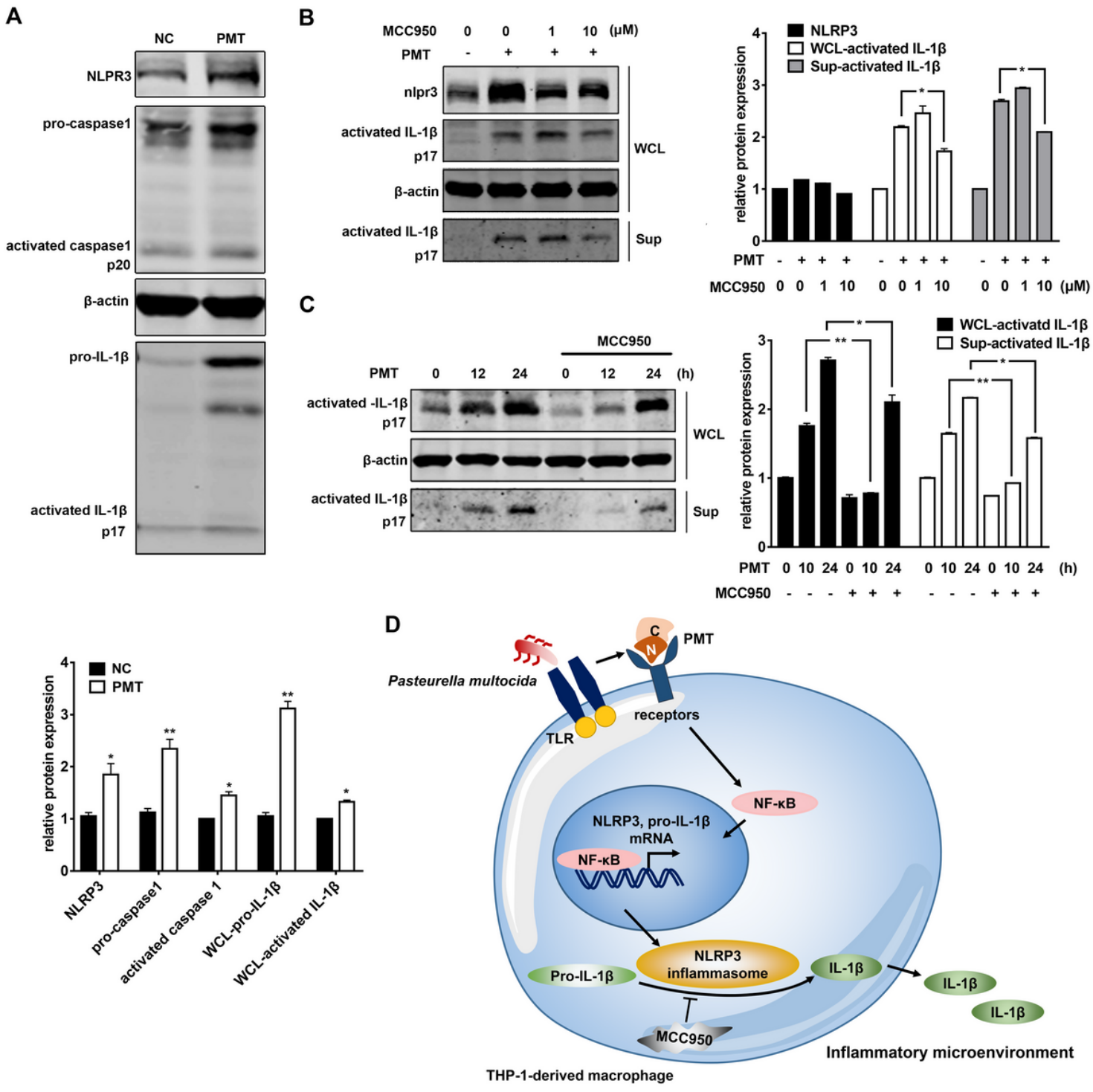

Figure 4

PMT activates NLRP3 inflammasome *in vitro.* (A) Protein expression of NLRP3, pro-caspase1, activated caspase1, pro-IL-1β, activated IL-1β and the internal control β-actin after stimulation of PMT for 12 h by western blot. The histogram shows the quantification of band intensities. β-actin was used for normalization relative to the control groups. (B) Protein expression of NLRP3, pro-IL-1β, activated IL-1β in whole cell lysates and supernatants and the internal control β-actin after stimulation of PMT with or without NLRP3 inhibitor MCC950 by western blot. The histogram shows the quantification of band

intensities. β-actin was used for normalization relative to the control groups. (C) Protein expression of activated IL-1β in whole cell lysates (WCL) and supernatants (Sup) and the internal control β-actin after stimulation of PMT with or without NLRP3 inhibitor MCC950 in a series of time by western blot. The histogram shows the quantification of band intensities. β-actin was used for normalization relative to the control groups. (D) Diagram illustrated that PMT can not only induce inflammatory reactions and the transcription of NLRP3 via the NF-κB signaling pathway, but also activate NLRP3 inflammasome with the release of activated IL-1β. NLRP3 inhibitor MCC950 can significantly reduce this effect. Values are presented as mean ± SD. (*p<0.05, **p<0.01). Abbreviations: IL = interleukin; mRNA = messenger RNA; NLRP3 = NOD-like receptor family pyrin domain containing 3; NF-κB = nuclear factor kappa light chain enhancer of B cells; PMT = *Pasteurella multocida* toxin.

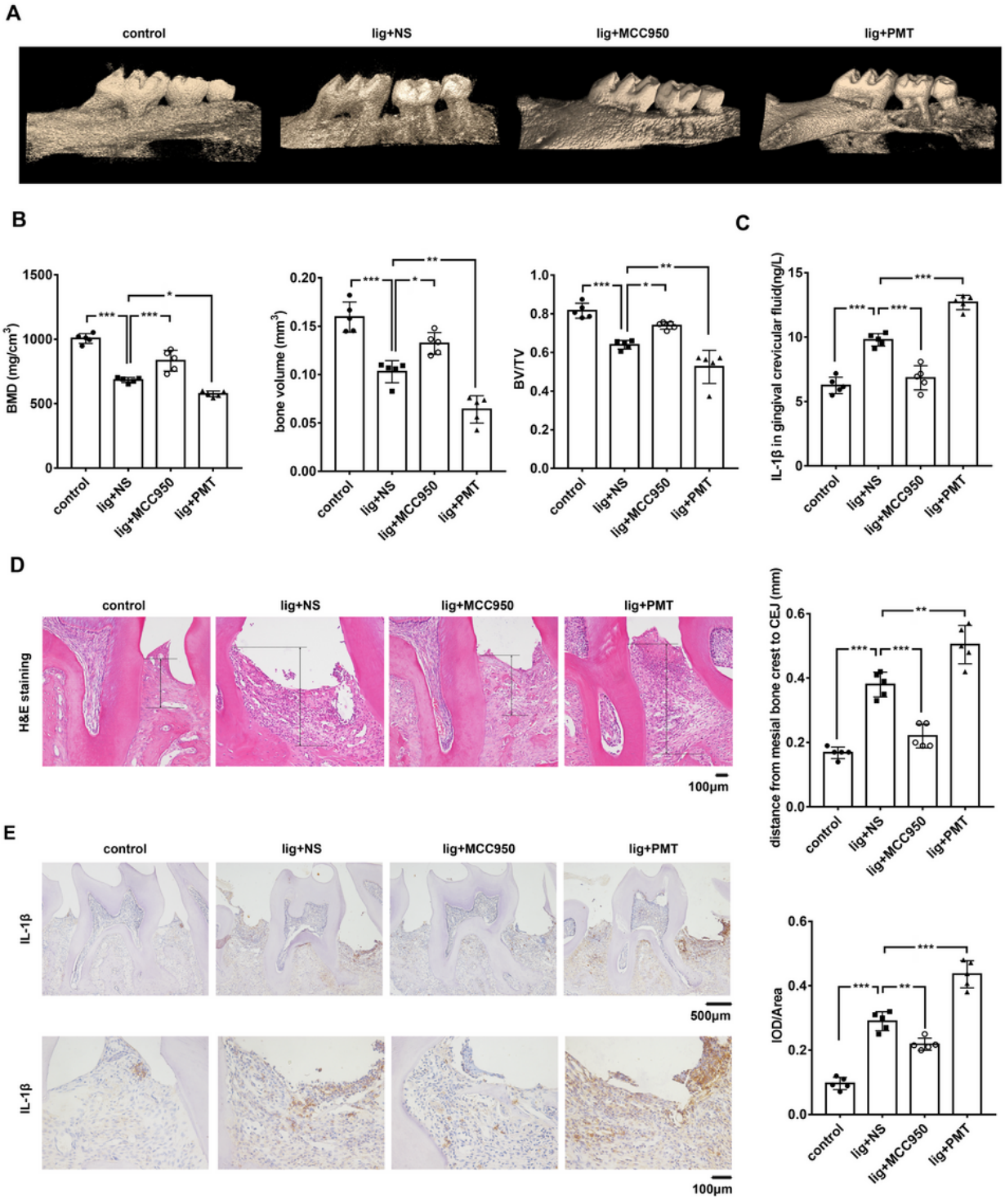

Figure 5

MCC950 ameliorates mice periodontitis while PMT aggravates mice periodontitis. (A) Reconstructed 3D micro-CT images of control, lig+NS, lig+MCC950, lig+PMT groups. (D) BMD, BV and BV/TV analysis of control, lig+NS, lig+MCC950, lig+PMT groups. (C) IL-1β protein expression in gingival crevicular fluid of control, lig+NS, lig+MCC950, lig+PMT groups. (D) H&E staining and the distances between the CEJ and the ABC from mesial side of f control, lig+NS, lig+MCC950, lig+PMT groups. (E) Immunohistochemistry

staining of IL-1β in the gingivae of control, lig+NS, lig+MCC950, lig+PMT groups. The histogram shows the quantification of average optical density (Integrated optical density (IOD)/Area) of IL-1β immunohistochemistry staining (n=5/group). Values are presented as mean ± SD. (*p<0.05, **p<0.01, ***p<0.001). Abbreviations: ABC = alveolar bone crest; BMD = bone mineral density; BV = bone volume; BV/TV = bone volume/tissue volume ratio; CEJ = cemento-enamel junction; H&E = hematoxylin and eosin; IL = interleukin; micro-CT = microcomputed tomography; NS = normal saline; PMT = *Pasteurella multocida* toxin; 3D = three-dimensional.

Supplementary Files

This is a list of supplementary files associated with this preprint. Click to download.

- appendix.docx